RSC Advances

ROYAL SOCIETY OF CHEMISTRY

www.rsc.org/advances

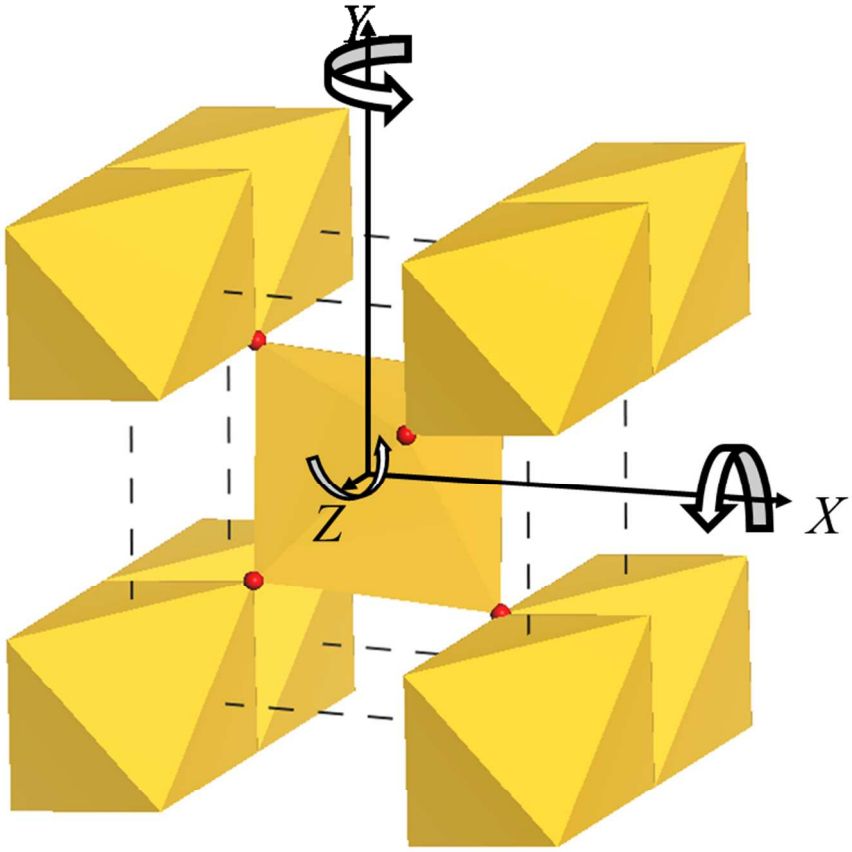

Journal Name

RSCPublishing

ARTICLE

Anomalous elastic properties in Stishovite

Cite this: DOI: 10.1039/xoxxoooooox

K. M. Azzopardi,[a] J. P. Brincat,[a] J. N. Grima[b] and Ruben Gatt[a]

Received ooth January 2012,
Accepted ooth January 2012

DOI: 10.1039/xoxxoooooox

www.rsc.org/

Auxetics are materials which have a negative Poisson's ratio, that is, upon uniaxial tensile loading, they also expand in a direction perpendicular to the applied force. Here, we analyze the elastic constants of stishovite, a high pressure silica polymorph which is known to be a significant constituent of the earth's mantle, and show that it exhibits negative Poisson's ratio when stressed in a range of directions in the (100), (010) and (001) planes at specific ambient pressure ranges. We explain this behaviour through mechanisms involving rotations and distortions of the constituting octahedra. These findings have important practical implications since stishovite is one of the hardest known oxides, and has proven to be important to various fields ranging from seismology to materials science.

Introduction

Stishovite, a rutile-type polymorph of SiO_2, is a hexa-coordinated tetragonal structure with a symmetry class of P42/mnm.[1-8] It was first synthesized more than half a century ago[9] before being discovered in nature,[1] an unusual sequence of events for a mineral which turned out to be so important to the fields of geophysics, solid state physics and chemistry.[5,10-14] The main reason for this is that stishovite is only formed at pressures which are several hundred thousand times higher than atmospheric pressure. Such pressures can be encountered in meteorite impacts[15] and in the Earth's mantle. In fact, studying the mechanical properties of stishovite as a function of pressure is essential since it may be a significant constituent of the Earth's mantle,[16-23] and accurate knowledge of the elastic moduli and the pressure dependence of the silicate polymorphs which compose the mantle is essential for seismology.[4,24] This has led to many studies being devoted to the determination of the mechanical properties of stishovite, including the experimental determination of its elastic constants at different pressures.[25] The interpretation of these experimentally determined constants however focused primarily on the stiffness properties of this material, namely its bulk moduli and shear moduli together with their pressure derivatives. For example, it was shown that the compressive strength of stishovite increases with increasing pressure,[4,6,8,25] while the shear modulus (C_{11}-C_{12}) seems to decrease with increasing pressure[4,6,8,25] eventually ending at a point of elastic instability which indicates a phase transition.[4,5,26]

In this work we focus on studying the Poisson's ratio of stishovite at different pressures, using both experimental data (as published in the literature[4,8,23,27,28]) as well as through DFT simulations. We show that the Poisson's ratio of stishovite is negative, i.e. the system is auxetic[28-31], for loading in specific directions in certain planes and at certain pressures. To the best of our knowledge, this important property of stishovite has been ignored so far, even if the Poisson's ratio of other naturally occurring silica polymorphs have been studied extensively.[32-37] One such example is the well-known auxetic α-cristobalite, which exhibits auxetic behaviour at atmospheric pressure. α-cristobalite is a silica polymorph from which stishovite may be produced by the application of pressure.[22,38]

Since auxeticity is known to be a function of the geometry and the deformation mechanism of a particular system, a detailed investigation into the mechanism which leads to such behaviour in stishovite was undertaken in order to better understand the negative Poisson's ratios observed. This was done through DFT simulations, by applying uniaxial stresses in the direction of minimum Poisson's ratio at different pressures.

Results and Discussion

The structure of stishovite, optimized at various pressures (0-30 GPa) using DFT calculations, and its mechanical properties, calculated using the constant-strain method, were compared to the experimental structure[39] and mechanical properties[4,8,24,27,28] published by various authors. Figure 1(a) compares the optimized fractional co-ordinates with the experimentally derived co-ordinates presented by Ross[39]. As can be seen in this Figure the results are practically identical. Figure 1(b) compares the off-axis Poisson's ratios calculated in this work with experimentally derived values available in literature. The calculated Poisson's ratios were found to coincide most closely with the ratios published by Holm,[28] though all the other published results follow the same trends very closely. The parameters computed at non-zero ambient pressure in this work are credible since they were calculated using the same method

for which excellent agreement was obtained with other published literature at ambient pressure.

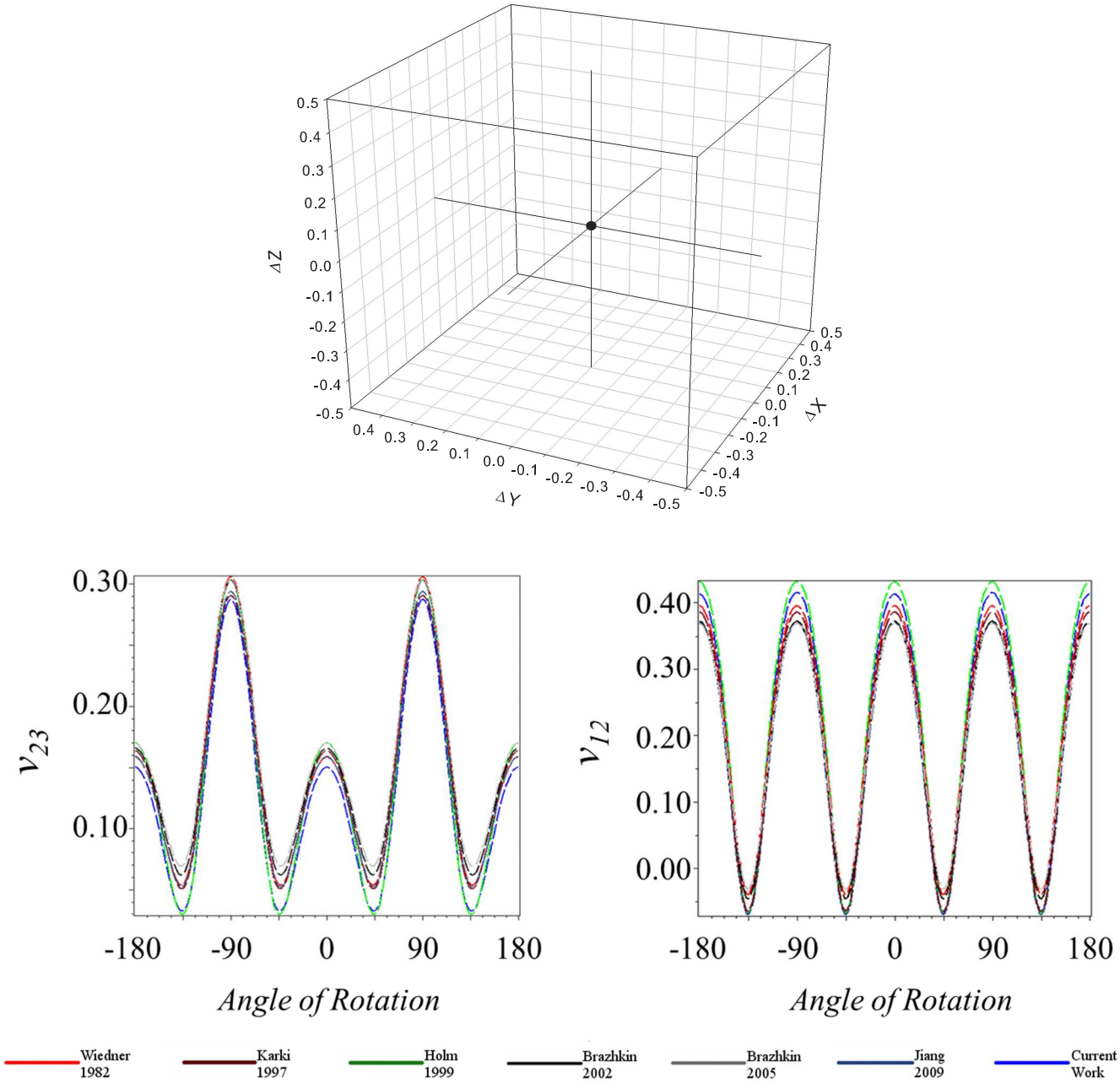

Figure 1: (a) (top) Comparison of the fractional coordinates of experimental and calculated structures. (b) (bottom) Plots for published data, compared to the results obtained in this work.

Changes in Poisson's ratio with increasing pressure

The plots in Figure 1(a) immediately highlight the high anisotropy of the system with respect to the Poisson's ratios. The full set of off-axis Poisson's ratios, calculated using standard axis transformation techniques, and their variation with pressure in the (001) plane and in the (100) plane are given in Figure 2. These results indicate that auxetic behaviour is present in the (001) plane of stishovite up to 30 GPa of ambient pressure. The minimum Poisson's ratio in this plane becomes gradually less negative as the external pressure increases, and is nearly zero at an ambient pressure of 30 GPa. The direction of

minimum Poisson's ratio is circa 45° throughout the ambient pressure range studied in this plane.

The opposite trend is observed in the (100) plane. In this case, the Poisson's ratios are positive at 0 GPa of ambient pressure, yet start decreasing as the ambient pressure is increased, as shown in Figure 2(b). The (010) plane is identical to the (100) plane.

In these planes, the minimum value obtained for the Poisson's ratio of circa -0.2 was observed at 30 GPa of ambient pressure. As this pressure is increased, the direction of the minimum Poisson's ratio, which is circa 45° to the [010] axis at 0 GPa, shifts to circa 49° at 30 GPa of ambient pressure.

It is interesting to note that the maximum Poisson's ratio does not change significantly with increasing pressure in the (100) and (010) planes, while the minimum Poisson's ratio varies greatly. On the other hand, in the (001) plane it is the minimum Poisson's ratio which does not change significantly with pressure, while the maximum Poisson's ratio undergoes wider changes.

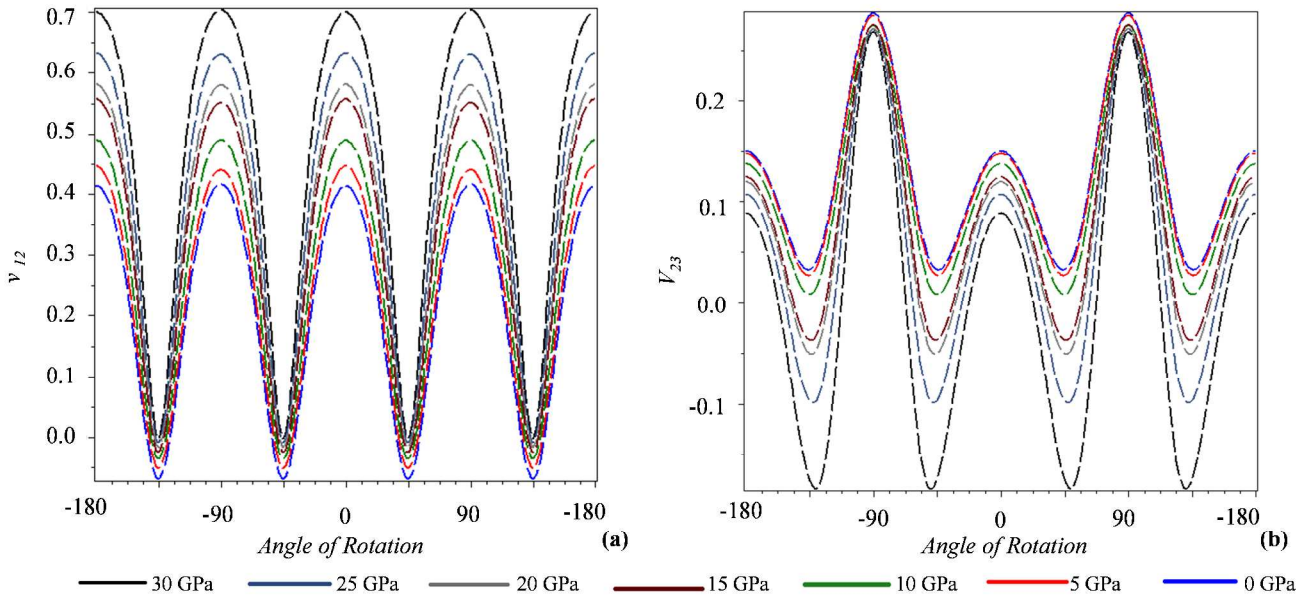

Figure 2: The off-axis Poisson's ratio and its variation with pressure in the (001) plane (v_{12}) and in the (100) plane (v_{23}). The (010) plane is identical to the (100) plane.

Changes in structure with increasing pressure

An analysis of how different geometric parameters of stishovite change with pressure is given in Figure 3, which shows both the reference frames used for the measurements taken, and plots of the results obtained. Note that the scale on the y-axis is very narrow, indicating that the measured changes are very subtle. This is due to the structure of stishovite already being very dense. X-ray diffraction spectra for three of the structures produced are included in the Supporting Information for clarity.

The two octahedra which compose the unit cell of stishovite undergo identical changes. As the ambient pressure increases, the octahedra distort, but they do not rotate relatively to each other.

The most significant distortion observed is the decrease in bond length, which is comparable to the changes incurred by the lattice parameters. Moreover, the axial bonds decrease in length more than the equatorial bonds, changing by circa 0.127% per GPa of ambient pressure. This makes both octahedra squatter.

The octahedral equatorial bonds also undergo a slight scissoring distortion on increasing ambient pressure. More specifically, referring to Figure 3(b), angles O_5-Si_1-O_6 and O_9-Si_2-O_{10} undergo a scissoring of 0.002° per GPa.

The decrease in bond length, scissoring distortion and lack of rotations are in stark contrast to the behaviour of α-cristobalite, another silicate with a negative Poisson's ratio, which deforms through tetrahedral rotation when subjected to a change in ambient pressure.[35]

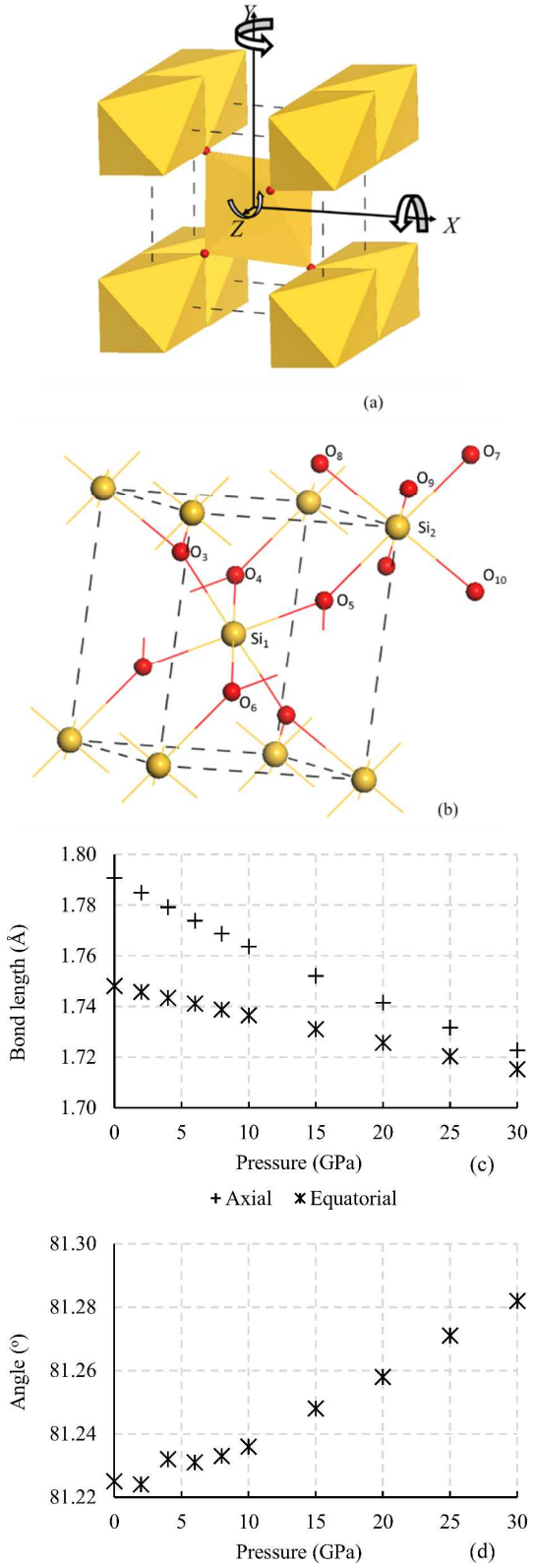

Figure 3: (a) Rotations around the three major axis for octahedron 1 in stishovite. (b) The labels used to measure the bond angles and bond lengths for the two octahedra in the unit cell of stishovite. (c) Variations in the bond lengths (left) and scissoring angle (right) as a function of increasing ambient pressure.

Deformation mechanisms for individual planes

Uniaxial stress was applied to the structure of stishovite in the (001) and (100) planes independently, along the direction of maximum auxeticity in the respective plane. As is generally the case with natural systems, when loaded uniaxially, stishovite deforms through a number of concurrent deformation mechanisms that bring about the observed physical properties. Some of these mechanisms act to produce a negative Poisson's ratio, while others lead to conventional behaviour.

Considering the (001) plane first, loading this plane in the direction of maximum auxeticity (45° to the [010] axis) causes the two octahedra which compose the unit cell to distort, but not to rotate relative to each other. Referring to Figures 3(a,b) and 4, the axial bonds of octahedron 1, which is aligned to the loading direction, stretch from 1.79 Å at 0 GPa of uniaxial stress to 1.80 Å at 1.22 GPa of uniaxial tensile stress. It is interesting to note that the axial bonds of the octahedra tend to stretch to a larger degree when compared to the equatorial bonds.

The stretching of the axial bonds is accompanied by a 'scissoring' distortion of the equatorial bonds, wherein the equatorial plane of octahedra 1 and 2 become more regular. This scissoring distortion, which is larger in octahedron 2, opens up the structure of stishovite in the direction perpendicular to the applied force, and results in the octahedra having a more rectangular conformation along the equatorial plane, while the equatorial bonds remain orthogonal to the axial bonds (see Figure 3(b)).

When considering how the deformation mechanism in this plane is changing as a function of ambient pressure, one notes that as the ambient pressure is increased, the scissoring distortion of octahedron 2 decreases on increasing uniaxial stress, while the scissoring distortion of octahedron 1 remains nearly constant. Recall that increasing the pressure induces a decrease in auxeticity in the (001) plane. This corroborates the hypothesis that the scissoring effect is responsible for the observed negative Poisson's ratio in this plane.

As uniaxial stress is applied in the direction of maximum auxeticity in the (100) and (010) planes (~45° to [010] in both planes), both octahedra distort and rotate relative to each other, as may be inferred from Figure 4. The rotations occur for each octahedron about all three major crystallographic axes, however rotations about the [001] axis are the most prominent. The distortions of the octahedra are of two main types: (1) scissoring of the equatorial bonds (angles O_5-Si_1-O_6 and O_9-Si_2-O_{10} in Figure 3(b)) and (2) bending of the axial bonds relative to the equatorial plane (angles O_3-Si_1-O_5, O_3-Si_1-O_5, O_9-Si_2-O_7 and O_8-Si_2-O_7 in Figure 3(b)). The scissoring behaviour of the equatorial bonds opens up the structure in the direction perpendicular to the applied force, giving rise, at least in part, to the observed negative Poisson's ratio. The bond lengths do not change significantly, with the maximum change in length never exceeding circa 0.7%.

Upon increasing the ambient pressure, (as the (100) and (010) planes becomes more auxetic) the rotations of the octahedra about the [001] axis and the scissoring distortions increase, while the rotations about the [100] and [010] axes remain constant on application of uniaxial stress. On the other hand the bending of the axial bonds decrease. This validates the proposed theory that these two deformation mechanisms are responsible for the observed negative Poisson's ratios in these planes.

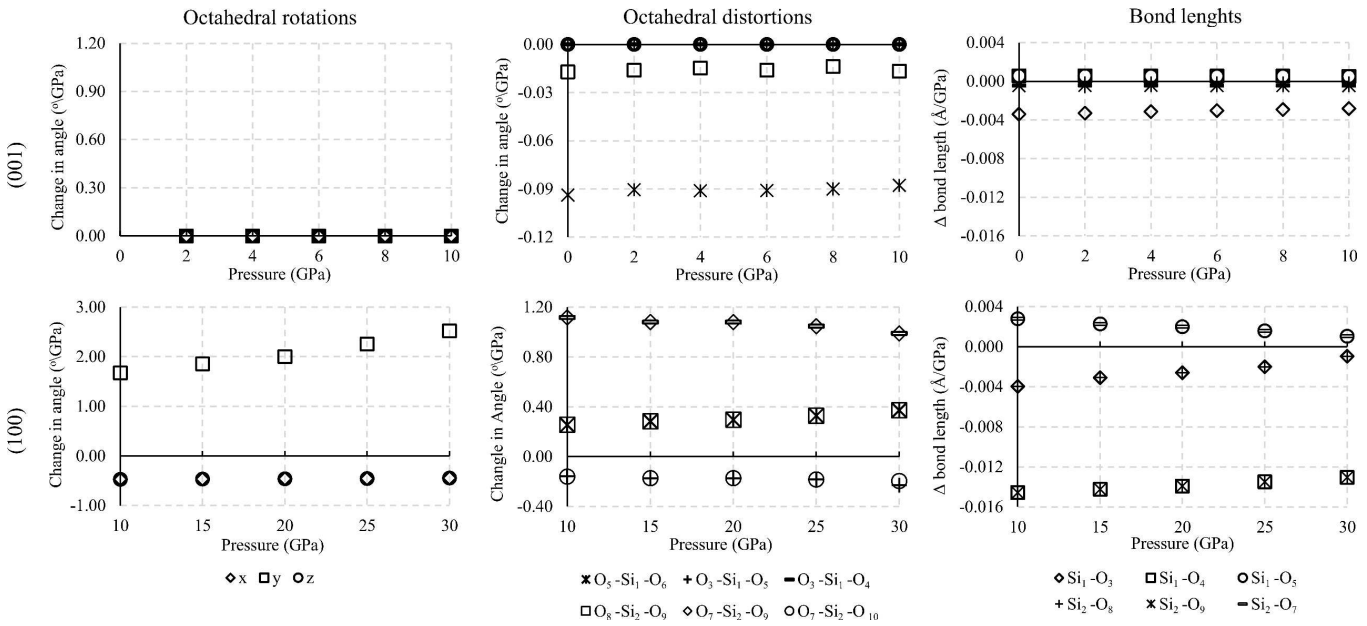

Figure 4 Measured variations in octahedral rotations, octahedral distortions and bond lengths in the (001) and (100) planes as a function of applied uniaxial stress in the direction of minimum Poisson's ratio in the respective plane.

Auxetic behaviour in three-dimensional stishovite.

Considering the 3D structure of stishovite as a whole, it is evident from the results obtained that octahedral deformations have an effect on the Poisson's ratios in all three orthogonal planes.

More importantly, scissoring distortions in particular have a significant effect on the Poisson's ratio. On increasing ambient pressure, these distortions arereduced when loading the (001) plane at 45° to the [010] axis. This results in the minimum Poisson's ratio in this plane becoming more positive. On the other hand, as the ambient pressure increases, the same scissoring distortions increase in relevance while loading the (100) plane at 45° to the [010] axis. In this case, the Poisson's ratio in this plane becomes more negative. Both these observations, when taken together, imply that scissoring distortions are a likely candidate for the cause of the observed auxetic behaviour in stishovite.

These octahedral deformations may be caused by electronic effects such as the Jahn-Teller effect, where the octahedral distortions would result in a lower energy of the system. Although such a hypothesis would need to be verified in subsequent studies, this would imply that the distortions of the octahedra and hence the observed Poisson's ratios, lead to a more energetically favourable system.

Before concluding, it is important to note that the data presented in Figures 3 and 4 all seem to fit within a trend. This is an indication that the data was collected from structures which are in local minima. It is also important to highlight that this work furthers the understanding of the ever growing list of exceptional properties of the crystal stishovite. The described mechanism of octahedral distortions and rotations results in a negative Poisson's ratio, and hence introduces auxeticity into the structure. This work also provides experimental chemists and crystal engineers designing novel metamaterials with a new deformation mechanism which gives rise to negative Poisson's ratios: the distortions of octahedra. These distortions may be used to produce materials with a negative Poisson's ratio, and hence facilitate the long-term goal of production of tunable structures.

Experimental Section

The structure of stishovite[39] was optimized at various pressures (0-30 GPa) using DFT calculations. These simulations were conducted using the CASTEP[40] program in the Material studios v6.1[41] package on a 1x1x1 unit cell, and periodic boundary conditions were used throughout. To minimize symmetry constraints apart from those imposed by the unit cell itself, the space group was set to P1 rather than P42/mnm. Removing of the symmetry constrains resulted in a significant increase in the computational time of the simulations, however this was a must for the current study as it was required that all elements of the cell act independently. Furthermore, geometry optimizations were conducted using the BFGS minimizer[42] as this allows for simultaneous relaxation of the internal degrees of freedom together with the cell parameters. Stringent convergence criteria were used as detailed in the Supporting Information. The cut off energy was found to be sufficient at 1000 eV. The Brillouin Zone sampling was conducted by means of a Monkhorst-Mesh grid[43] with 4x4x6 spacing. Norm conserving pseudopotentials were used for the simulations as included in the Material Studios package. The performance of two Generalized Gradient Approximation (GGA) functionals (GGA-PBE and GGA-PW91) and the Local Density Approximation (LDA) functional was tested. Results showed that these functionals all required similar energy cut-offs and mesh sampling to converge (see Supporting Information). The LDA functional was therefore selected for subsequent calculations since the GGA techniques are more computationally intensive while producing similar results. Furthermore, the converged setting for both the GGA functionals seemed to have a greater deviation from the experimental values that those obtained through the LDA calculations (see Supporting Information).

The elastic constants were then calculated at each pressure by applying the constant-strain method, which involves applying a

series of normal strains and shear strains, measuring the respective stress, and using standard transformations to produce the stiffness matrix (the full set of elastic constants). From this matrix, the off-axis plots at the respective pressures were calculated and the angles of maximum and minimum auxeticity were obtained.

The calculated elements of the stiffness matrix [**C**] were compared to those available in published literature[4,8,24,27,28] (0-12 GPa), and were found to coincide. The structures obtained were also nearly identical. Using standard axis transformation techniques as discussed elsewhere,[44,45] the Poisson's ratio properties of stishovite were then calculated. This was done in order to identify the deformation mechanisms which lead to auxeticity. Note that other novel methods, such as those published by Bosak and co-authors,[46] can also be used to study materials under high pressure.

Further simulations were performed in order to elucidate the deformation mechanism in the direction of maximum auxeticity in the (100) and (001) planes. The (001) plane was investigated between 0 and 10 GPa of external pressure at 2 GPa intervals, since the Poisson's ratio of stishovite was found to be significantly negative between these limits. The (100) plane was studied between 10 and 30 GPa of external pressure at 5 GPa intervals for the same reason. In each additional simulation, the structures were once again subjected to a series of geometry optimizations when being stressed by up to 0.2% of the Young's modulus in the direction of minimum Poisson's ratio. Detailed measurements of bond lengths, bond angles and inter-atom distances were obtained to study the deformation mechanisms.

Conclusions

We have shown that stishovite may exhibit negative Poisson's ratios for loading off-axis, a property which becomes more prominent as the ambient pressure is increased in the (100) and (010) planes, and less prominent in the (001) plane. It has been observed that the region of lowest Poisson's ratio also shifts in direction in the (001) and (010) planes upon increasing pressure. It was found that in the case of stishovite, octahedral distortions play an important part vis-a-vis the observed negative Poisson's ratio. This novel deformation mechanism represents an advance in the field since all the conclusions presented here may be transferred to other rutile structures and structures made of octahedra and tetrahedra.

Acknowledgements

This research has been carried out using computational facilities procured through the European Regional Development Fund, Project ERDF-080 'A Supercomputing Laboratory for the University of Malta'

Notes and references

[a] Metamaterials Unit, Faculty of Science, University of Malta, Msida, MSD 2080.

[b] Department of Chemistry, Faculty of Science, University of Malta, Msida, MSD 2080.

1 E. C. T. Chao, J. J. Fahey, J. Littler and D. J. Milton, *Geophys. Res.*, 1962, **67**, 419.

2 W. Sinclair and A. E. Ringwood, *Nature*, 1978, **272**, 714.

3 F. Liu, H. Garofalini, D. King-Smith and D. Vanderbilt, *Phys. Rev. B*, 1994, **49**, 12528.

4 B. B. Karki, L. Stixrude and J. Crain, *Geophys. Res. Lett.*, 1997, **24**, 3269.

5 M. A. Carpenter, R. J. Hemley and H. Mao, *J. Geophys. Res.*, 2000, **105**, 10807.

6 S. R. Shieh, T. S. Duffy and B. Li, *Phys. Rev. Lett.*, 2002, **89**, 255507.

7 T. Yamanaka, T. Fukuda and J. Tsuchida, *Phys. Chem. Miner.*, 2002, **29**, 633.

8 F. Jiang, G. D. Gwanmesia, T. I. Dyuzheva and T. S. Duffy, *Phys. Earth Planet. Inter.*, 2009, **172**, 235.

9 S. M. Stishov and S. V. Popova, *Geokhimiya*, 1961, **10**, 837.

10 K. J. Kingma, R. E. Cohen, R. J. Hemley and H. Mao, *Nature*, 1995, **374**, 243.

11 C. Lee and X. Gonze, *J. Phys. Condens. Matter*, 1995, **7**, 3693.

12 D. Andrault, G. Fiquet, F. Guyot and M. Hanfland, *Science*, 1998, **282**, 720.

13 D. M. Teter, R. J. Hemley, G. Kresse and J. Hafner, *Phys. Rev. Lett.*, 1998, **80**, 2145.

14 V. V. Brazhkin, L. E. McNeil, M. Grimsditch, N. A. Bendeliani, T. I. Dyuzheva and L. M. Lityagina, *J. Phys. Condens. Matter*, 2005, **17**, 1869.

15 I. P. Baziotis, Y. Liu, P. S. DeCarli, H. J. Melosh, H. Y. McSween, R. J. Bodnar and L. A. Taylor, *Nat. Comm.*, 2013, **4**, 1404.

16 W. A. Bassett and J. D. Barnett, *Phys. Earth Planet. Inter.*, 1970, **3**, 54.

17 R. C. Liebermann, A. E. Ringwood and A. Major, *Earth Planet. Sci. Lett.*, 1976, **32**, 127.

18 T. Yagi and S.-I. Akimoto, *Tectonophysics*, 1976, **35**, 259.

19 C. Lee and X. Gonze, *Phys. Rev. Lett.*, 1994, **72**, 1686.

20 B. Li, S. M. Rigden and R. C. Liebermann, *Phys. Earth Planet. Inter.*, 1996, **96**, 113.

21 E. A. Goresy, L. Dubrovinsky, T. G. Sharp, S. K. Saxena and M. Chen, *Science*, 2000, **288**, 1632.

22 L. Huang, M. Durandurdu and J. Kieffer, *Nat. Mater.*, 2006, **5**, 977.

23 A. Verma and B. Karki, *Phys. Rev. B*, 2009, **79**, 214115.

24 D. J. Weidner, J. D. Bass, A. E. Ringwood and W. Sinclair, *J. Geophys. Res.*, 1982, **87**, 4740.

25 A. K. Singh, D. Andrault and P. Bouvier, *Phys. Earth Planet. Inter.*, 2012, **208-209**, 1.

26 A. P. Cordier, A. D. Mainprice and J. L. Mosenfelder, *Eur. J. Mineral.*, 2004, **16**, 387

27 V. V. Brazhkin, M. Grimsditch, I. Guedes, N. A. Bendeliani, T. I. Dyuzheva and L. M. Lityagina, *Phys.-Usp.*, 2002, **45**, 447.

28 B. Holm and R. Ahuja, *J. Chem. Phys.*, 1999, **111**, 2071.

29 J. N. Grima, R. Jackson, A. Alderson and K. E. Evans, *Adv. Mater.*, 2000, **12**, 1912.

30 J. N. Grima, R. Gatt, N. Ravirala, A. Alderson and K. E. Evans, *Mater. Sci. Eng. A*, 2006, **423**, 214.

31 F. Scarpa, S. Blain, T. Lew, D. Perrott, M. Ruzzene and J. R. Yates, *Compos. Part A Appl. Sci. Manuf.*, 2007, **38**, 280.

32 R. Gatt, D. Attard, P.-S. Farrugia, K. M. Azzopardi, L. Mizzi, J.-P. Brincat and J. N. Grima, *Phys. Status Solidi B*, 2013, **250**, 2012.

33 A. Yeganeh-haeri, D. J. Weidner and J. B. Parise, *Science*, 1992, **257**, 650.

34 H. Kimizuka, H. Kaburaki and Y. Kogure, *Phys. Rev. Lett.*, 2000, **84**, 5548.
35 H. Kimizuka, S. Ogata, Y. Shibutani, *Mater. T. JIM.*, 2005, **46**, 1161.
36 A. Alderson and K. E. Evans, *Phys. Rev. Lett.*, 2002, **89**, 225503.
37 J. N. Grima, R. Gatt, A. Alderson and K. E. Evans, *Mater. Sci. Eng. A*, 2006, **423**, 219.
38 D. D. Klug, R. Rousseau, K. Uehara, M. Bernasconi, Y. Le Page and J. Tse, *Phys. Rev. B*, 2001, **63**, 104106.
39 N. L. Ross, J. F. Shu, R. M. Hazen and T. Gasparik, *Am. Mineral.*, 1990, **75**, 739.
40 S. J. Clark, M. D. Segall, C. J. Pickard, P. J. Hasnip, M. I. J. Probert, K. Refson and M. C. Payne, *Z. Kristallogr.*, 2005, **220**, 567.
41 Materials Studio is commercialized by Accelrys®. http://accelrys.com/
42 B. G. Pfrommer, M. Cote, S. G. Louie, and M. L. Cohen, *J. Comput. Phys.*, 1997, **131**, 233.
43 H. J. Monkhorst and J. D. Pack, *Phys. Rev. B*, 1976, **13**, 5188; H. J. Monkhorst and J. D. Pack, *Phys. Rev. B*, 1977, **16**, 1748.
44 J. F. Nye, *Physical properties of crystals*, 1957, Clarendon, Oxford.
45 J. N. Grima, *Ph.D. thesis*, 2000, University of Exeter.
46 A. Bosak, I. Fischer, M. Krisch, V. Brazhkin, T. Dyuzheva, B. Winkler, D. Wilson, D. Weidner, K. Refson and V. Milman, *Geophys. Res. Lett.*, 2009, **36**, L19309.